



PERGAMON

Vacuum 64 (2002) 287–291

VACUUM
SURFACE ENGINEERING, SURFACE INSTRUMENTATION
& VACUUM TECHNOLOGY

www.elsevier.com/locate/vacuum

Structural and optical characterization of WO₃ deposited on glass and ITO

A. Monteiro^a, M.F. Costa^a, B. Almeida^{a,*}, V. Teixeira^a, J. Gago^b, E. Roman^b

^aDepartamento de Física, Universidade do Minho, Largo do Paço, 4710-057 Braga, Portugal

^bICMM-Instituto de Ciencia de Materiales, CSIC, Cantoblanco, Madrid, Spain

Abstract

Electrochromic materials exhibit variable and reversible optical properties under the action of voltage pulses. The interest in these materials has increased in the last few years due to their potential application in a wide variety of optical modulation devices. Tungsten oxide (WO₃) is typical in such devices. In this work, we present a study of the structural and optical properties of tungsten oxide films deposited on glass and indium tin oxide. The films were produced by reactive dc magnetron sputtering at different temperatures (room temperature and 200°C) and bias voltage (−60 to +60 V). The sputtering atmosphere was composed of an Ar + O₂ mixture so that sample could be deposited with different oxygen partial pressure ($0.2 \leq p(\text{O}_2) \leq 0.8$). Spectral transmission in the visible and near infrared was measured using a double-beam spectrophotometer. X-ray diffraction was used in order to characterize the film structure. The surface microtopography was analyzed by atomic force microscopy (AFM). XRD results show that for low $p(\text{O}_2)$ the films present an amorphous WO₃ phase, while for high oxygen partial pressure they present a mixture of a more crystalline WO₃ phase and a W₂₀O₅₈ phase. The structure change is for $p(\text{O}_2) = 0.5$ – 0.6 . A corresponding minimum was observed in the transmission and in the optical band gap, at these oxygen partial pressures. These results show that the optical properties of the films are dependent on the presence of oxygen deficient regions on the films. This was also observed in the samples deposited with an applied bias voltage. Microstructure (AFM) and X-ray measurements in these samples show that electron bombardment (positive bias) favors crystallinity and ion bombardment (negative bias) favors amorphization of the tungsten oxide phases present on the films. © 2002 Elsevier Science Ltd. All rights reserved.

Keywords: Tungsten oxide; Optical properties; Reactive magnetron sputtering

1. Introduction

Electrochromic thin films are of considerable technological interest due to their potential application on “smart-windows” [1–3], automobile mirrors [4], low-refractive materials in filters [5] and non-emissive displays. Electrochromism can

be described by a reversible change in transmittance and/or reflectance, caused by an applied external voltage [6,7]. To observe this change, it is necessary to incorporate the electrochromic layer in an electrochromic device [8]. The device consists of an electrochromic and ion storage layer separated by an ion-conducting layer [8]. Two external transparent conducting layers are used to apply the voltage. Tungsten oxide is one of the most studied electrochromic material [9,10] and it

*Corresponding author. Fax: +351-253-678981.

E-mail address: bernardo@fisica.uminho.pt (B. Almeida).

can be prepared by RF sputtering [11], CVD [12], sol–gel [10], thermal evaporation [13] and reactive direct-current (DC) magnetron sputtering [14]. Depending on the deposition conditions and techniques films may present considerably different structural, optical and electrical behaviour, and consequently different electrochromic behaviour [3,4]. With DC sputtering from a compressed target, thin film properties can be improved by controlling the reactive gas atmosphere. In this work, we present a study of the structural and optical properties of WO_3 films deposited by reactive magnetron sputtering on glass and indium tin oxide (ITO) coated glass. The deposition was performed at different oxygen partial pressures, both at room temperature and 200°C . The effect of applying a bias voltage to the ITO layer during WO_3 deposition was also studied.

2. Experimental

Tungsten oxide films were prepared by DC reactive magnetron sputtering on microscope slide glass and ITO coated glass (Delta Technologies, Ltd), both at room temperature and 200°C . The target was composed of a compressed tungsten powder with 99.95% purity. Sputtering was done with an atmosphere of $\text{Ar} + \text{O}_2$ gas mixture that was kept at a 1.3×10^{-2} mbar total work pressure in all cases. However, the partial pressure of oxygen ($p(\text{O}_2) = P(\text{O}_2)/[P(\text{O}_2) + P(\text{Ar})]$) was varied between 0.2 and 0.8 in our study. The Ar and O_2 gas purity was better than 99.99%. Electron and ion bombardment of the films was achieved by applying a bias potential (U_{bias}) to the ITO coated glass substrate during deposition. The bias voltage ranged from -60 to $+60$ V. ITO sheet resistance was $30 \pm 10 \Omega$. To remove any contamination, the substrates were cleaned with alcohol and the target was pre-sputtered before deposition. The thickness of the WO_3 thin films was calculated by the Swanepoel method [15] and it ranged between 360 and 570 nm.

Optical characterization was done using a double-beam UV–VIS–NIR spectrophotometer with automatic data acquisition. The analyzed wavelength ranged from 300 to 2300 nm. The

deposition rate of oxide films estimated from the thickness and deposition time ranged between 7–30 Å/min, depending on the oxygen concentration on the sputtering atmosphere. To characterize the film structure, X-ray diffraction studies were performed using a Philips PW-1710 diffractometer operating with Cu K_α radiation. Atomic force microscopy (AFM) using a digital instruments nanoScope in no contact mode was used in order to analyze the surface microtopography.

3. Results and discussion

Figs. 1a and b show typical X-ray diffraction spectra measured on the tungsten oxide films. It is observed that films deposited with low oxygen partial pressure ($p(\text{O}_2) \leq 0.5$), at room temperature and 200°C , present an amorphous WO_3 phase with peaks near 25.96 (001), 35.02 (021) and 53.80 (002). However, as $p(\text{O}_2)$ increases the structure of the films start to change so that for $p(\text{O}_2) \geq 0.5$ the films present a mixture of a more crystalline WO_3 phase and a $\text{W}_{20}\text{O}_{58}$. To determine the oxygen concentration where the $\text{W}_{20}\text{O}_{58}$ starts to appear, we have drawn in Fig. 2, the relative X-ray intensity of the peaks for each sample as a function of the oxygen partial pressure. It is observed that at room temperature the curve presents a minimum at $p(\text{O}_2) = 0.6$ indicating the structural change. This effect is enhanced for higher deposition temperatures as shown in Fig. 2b for $T_{\text{dep}} = 200^\circ\text{C}$. Here the transition occurs for $p(\text{O}_2) = 0.5$, where the $\text{W}_{20}\text{O}_{58}$ peaks start to appear.

Fig. 3a shows typical spectral transmittance measured on the tungsten oxide samples. Films with an oxygen partial pressure between 0.3 and 0.8, present a transmittance near 80%. This high value in the visible range is due to the wide optical band gap of WO_3 . For $p(\text{O}_2)$ lower than 0.3, the transmission is strongly reduced due to the formation of metallic tungsten on the films. For oxygen concentrations higher than 0.8, sputtering was not possible due to excess of oxygen on the sputtering atmosphere. The effect of temperature in the transparency of the films is small.

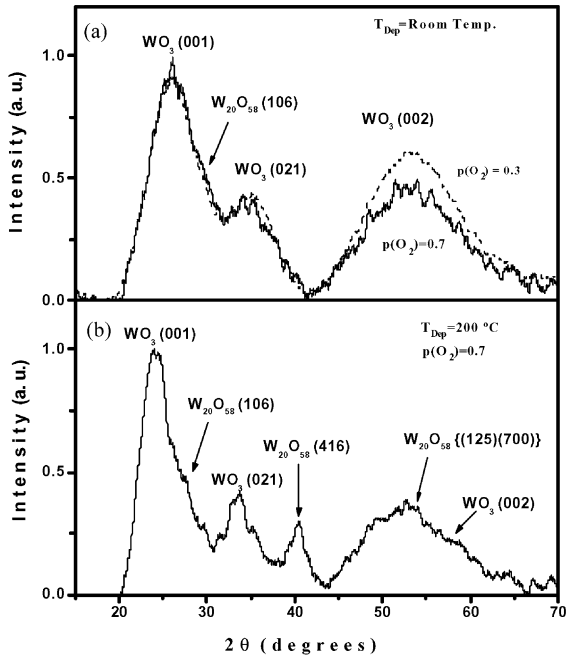


Fig. 1. X-ray diffraction spectra measured on the tungsten oxide films deposited at (a) room temperature and (b) 200°C.

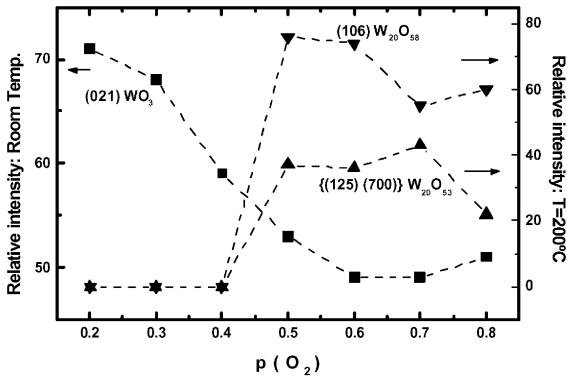


Fig. 2. Relative diffraction peak intensities of the phases present on the tungsten oxide films.

From the measured transmission spectra it was possible to obtain the absorption coefficient (α), using the method described in [15,16]. In amorphous semiconductors, assuming parabolic valence and conduction bands, the absorption coefficient near the absorption edge is given by $\alpha(h\omega) = B(h\omega - E_g)^2/h\omega$, where E_g is the band gap. From the absorption data, it was then

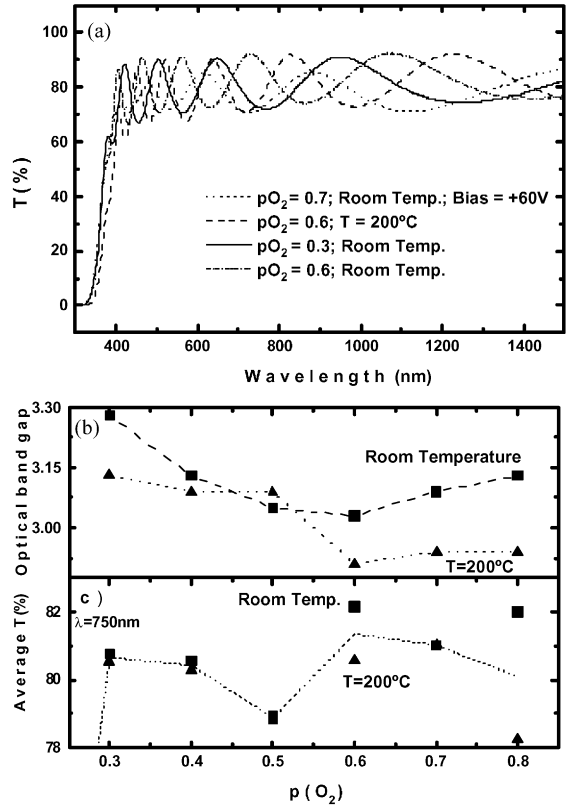


Fig. 3. Optical properties of the tungsten oxide films: (a) spectral transmittance; (b) bandgap and (c) average transmission at $\lambda = 750$ nm.

possible to obtain E_g for each film, and the values are plotted in Fig. 3b. It is observed that the optical band gap decreases with increase in oxygen partial pressure, attaining a minimum at $p(O_2) \sim 0.5-0.6$ and then increasing again. By plotting the average transmittance (without oscillations) at a particular wavelength as a function of the oxygen partial pressure it is also observed a minimum at $p(O_2) \sim 0.5-0.6$, both for films deposited at room temperature and 200°C (Fig. 3c).

The X-ray data already discussed show that for low oxygen partial pressure ($p(O_2) \leq 0.5$) the films lack oxygen to stabilize a well crystallized WO_3 phase. Also, for high oxygen partial pressure the WO_3 phase is more ordered, but a $W_{20}O_{58}$ oxygen deficient phase is increasingly present. Thus, the transmission and band gap results indicate that the optical properties are mainly controlled by the

presence of an oxygen deficient phase, and its amount on the films.

In order to optimize the properties of the WO_3 films, a bias potential U_{bias} was applied to the ITO coated glass substrate during deposition. Fig. 4 shows a characteristic surface microtopography of three films prepared by sputtering at room temperature ($p(\text{O}_2)=0.7$) with different applied bias voltage (-60 , 0 and $+60$ V). If U_{bias} is positive, then the electrons and negative ions bombard the surface. If U_{bias} is negative the surface is bombarded by positive ions. Since the physical effects of ion bombardment are expected to be independent of its charge and the photographs show different surface topography for positive and negative U_{bias} , this indicates that for positive applied voltages the bombardment is essentially from electrons.

Fig. 4a shows that for electron bombardment, the surface is very rough with bumps originated

from the columnar growth of the films. The bump height is 20 nm and their average separation is $0.1 \mu\text{m}$. Also, the electron bombardment of the surface gives energy to already deposited atoms so that they can diffuse to occupy crystal positions. Thus, these films are more crystalline as observed in the X-ray spectrum of Fig. 5a obtained on a film deposited at room temperature with $+60$ V bias voltage. This spectrum shows that the film presents a WO_3 phase with an increased crystallinity (smaller peak width) as compared to the corresponding film deposited with no bias voltage (Fig. 1a).

On the other hand, ion bombardment (negative voltages) disrupts the columnar structure and promotes denser and smooth films [17]. This induces the formation of a smooth surface as observed in Fig. 4c for the film deposited with $U_{\text{bias}} = -60$ V. Also, the X-ray spectrum measured on this film (Fig. 5b) show that this bombardment

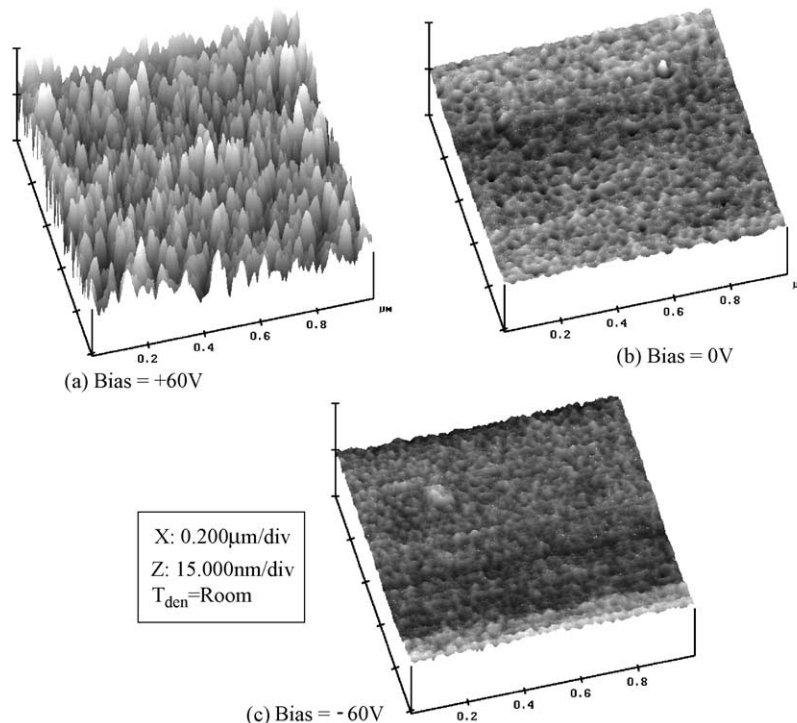


Fig. 4. Surface microstructure measured with AFM on films deposited at room temperature ($p(\text{O}_2)=0.7$) with an applied bias voltage: (a) $U_{\text{bias}} = +60$ V; (b) $U_{\text{bias}} = 0$ V; and (c) $U_{\text{bias}} = -60$ V.

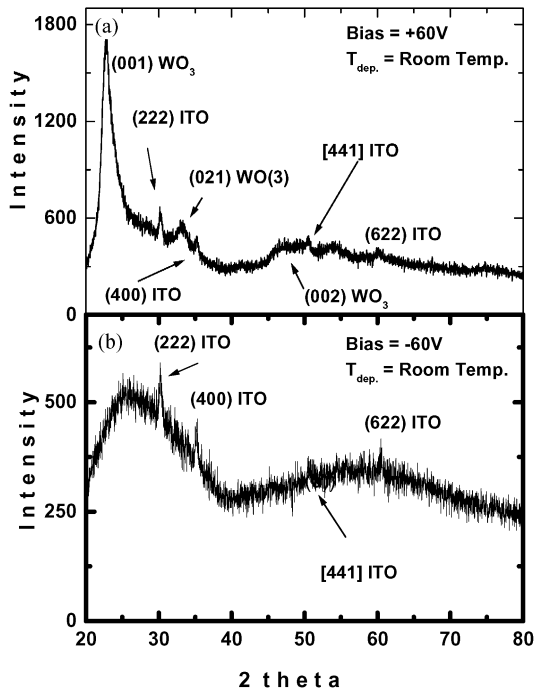


Fig. 5. X-ray diffraction spectra measured on the tungsten oxide films deposited at room temperature ($p(\text{O}_2)=0.7$) with an applied bias voltage: (a) $U_{\text{bias}} = +60$ V; and (b) $U_{\text{bias}} = -60$ V.

induces an increased amorphisation of the tungsten oxide as compared to the corresponding films deposited with no bias voltage (Fig. 1a).

The effect of electron and ion bombardment is not so sharp on the optical properties of the films. Their transmission spectra is similar both for positive and negative U_{bias} , attaining values near 80% in the optical region. However, the films deposited with positive polarization (electron bombardment) exhibit slightly lower transmission near the absorption edge ($\lambda < 400$ nm), as shown in Fig. 3a. This is an indication that the band gap E_g has decreased slightly for films deposited with these polarizations. Since the X-ray data show an increase in crystallinity of the WO_3 phase for positive U_{bias} , this indicates a reduction of oxygen deficient regions in these films.

In conclusion, the results on the tungsten oxide films show that for low $p(\text{O}_2)$ they present an amorphous WO_3 phase, while for high oxygen

partial pressure they present a mixture of a more crystalline WO_3 phase and a $\text{W}_{20}\text{O}_{58}$ oxygen deficient phase. The structure change is for $p(\text{O}_2)=0.5-0.6$. The optical measurements also show a minimum in transmission and optical band gap at these oxygen partial pressures. This indicates that the optical properties are dependent on the presence of oxygen deficient regions in the films. This result was also observed in the samples deposited with an applied bias potential. In these films, the AFM and X-ray measurements show that electron bombardment favors crystallinity and ion bombardment favors amorphisation of the tungsten oxide phases present in the films.

References

- [1] Antonaia A, Polichetti T, Addonizio ML, Aprea S, Minarini C, Rubino A. *Thin Solid Films* 1999;354:73.
- [2] DeVries MJ, Trimble C, Tiwald TE, Thompson DWJ. *Vac Sci Technol A* 1999;17:2906.
- [3] Lee KD. *Thin Solid Films* 1997;302:84.
- [4] Djourelou N, Gogova D, Misheva M. *Thin Solid Films* 1999;347:02.
- [5] Wagner W, Rauch F, Feile R, Ottermann C, Bange K. *Thin Solid Films* 1993;233:228.
- [6] Papaefthimiou S, Leftheriotis G, Yianoulis P. *Thin Solid Films* 1999;343–344:183.
- [7] Porcheras I, Vieira G, Martí J, Bertran E. *Thin Solid Films* 1999;343–344:179.
- [8] Goldner RB, Haas TE, Seward G, Wong K, Norton P, Foley G, Berera G, Wei G, Schulz S, Chapman R. *Solid State Ion* 1988;28–30:1715.
- [9] Trimble C, DeVries M, Hale JS, Thompson DW, Tiwald TE, Woolam JA. *Thin Solid Films* 1999;355–356:26.
- [10] Bedja I, Hotchandani S, Carpentier R, Vinodgopal K, Kamat PV. *Thin Solid Films* 1994;247:195.
- [11] Kaneko H, Nishimoto S, Miyake K, Suedomi NJ. *Appl Phys* 1986;59:2526.
- [12] Zhang Y, Wessel SA, Colbow K. *Thin Solid Films* 1990;185:265.
- [13] Ashrit PV, SPIE—Colorado 1999;3789:158.
- [14] Mo Y, Dillon RO, Snyder PG. *J Vac Sci Technol A* 1999;17:2933.
- [15] Swanepoel R. *J Phys* 1983;16:1214.
- [16] Gonzalez-Leal JM, Ledesma A, Bernal-Oliva AM, Prieto-Alcón R, Marquez E, Angel JA, Carabe J. *Mater Lett* 1999;39:2321.
- [17] Johnson PC. In: Vossen JL, Kern W, editors. *Thin film processes II*. San Diego: Academic Press 1991.